Journal of Physics B: Atomic, Molecular and Optical Physics

PAPER

Investigation of isolated attosecond pulse reconstruction from angular integrated photoelectron streaking spectra

To cite this article: Xi Zhao *et al* 2020 *J. Phys. B: At. Mol. Opt. Phys.* **53** 154002

IOP Publishing Journal of Physics B: Atomic, Molecular and Optical Physics
J. Phys. B: At. Mol. Opt. Phys. **53** (2020) 154002 (10pp) https://doi.org/10.1088/1361-6455/ab894d

Investigation of isolated attosecond pulse reconstruction from angular integrated photoelectron streaking spectra

Xi Zhao[1,2], Changli Wei[3,5], Su-Ju Wang[2], Bincheng Wang[1,4] and C D Lin[2]

[1] School of Physics and Information Technology, Shaanxi Normal University, Xian, Shaanxi 66506, People's Republic of China
[2] Department of Physics, Kansas State University, Manhattan, KS 66506, United States of America
[3] School of Physics and Electronics, Qiannan Normal College for Nationalities, Duyun, Guizhou 558000, People's Republic of China
[4] School of Physics and Wuhan National Laboratory for Optoelectronics, Huazhong University of Science and Technology, Wuhan 430074, People's Republic of China

E-mail: weicl11@163.com

Received 19 December 2019, revised 3 April 2020
Accepted for publication 15 April 2020
Published 23 June 2020

Abstract

We theoretically investigate the temporal characterization of isolated attosecond pulses from angular integrated photoelectron streaking spectra. In this work, our recently developed 'phase retrieval of broadband pulses' (PROBP) algorithm for attosecond pulse retrieval is modified so that photoelectrons emitted over a broad angular range can be used to retrieve the spectral phase of the broadband XUV to x-ray attosecond pulses. Compared to common retrieval methods that utilize photoelectrons only in the forward direction, the inclusion of electrons over a broad angular range has the advantage that stronger signals are analyzed to mitigate the effect of low statistics of photoelectrons for analysis. The present investigation also serves to test the commonly used approximation where the photoelectrons are collected over a finite angular range experimentally, but the theoretical analysis relies on electrons emitted only in the forward direction. Our results show that the extended PROBP method can be used to more accurately retrieve the spectral phase of an attosecond pulse from photoelectrons collected over a wider angular range.

Keywords: attosecond reconstruction, ultrafast dynamics, photonionization

(Some figures may appear in colour only in the online journal)

1. Introduction

With the advent of attosecond pulse trains (APTs) and isolated attosecond pulses (IAPs) since 2001 [1–4], attosecond (as) pulses have been used to study electron dynamics in photoionization [5], Auger decay [2], or charge migration in pump-probe experiments [6]. All of these phenomena occur on an attosecond timescale, and thus the temporal characterization of an attosecond pulse is required. In the recent decade, using long-wavelength driving lasers, through high-order harmonic generations, photon energy reaching 1.6 keV has been reported, with spectral width that can support attosecond pulses with duration of few attoseconds or even zeptoseconds if the pulses are transform-limited [7–17]. Yet so far only very few experiments actually have reported the determination of the pulse duration or the spectral phase of broadband attosecond pulses.

The difficulty of attosecond pulse characterization is well known. To determine the spectral phase, one would perform attosecond streaking experiments, where noble gas atoms are ionized by the XUV field in the presence of a moderately intense IR laser. With tunable time delays between the two

[5] Author to whom any correspondence should be addressed.

collinear beams, a two-dimensional photoelectron spectrogram or streaking traces are generated. While the spectral amplitude can be directly retrieved from the XUV-alone photoelectron spectra, to retrieve the spectral phase, one would have to use the streaking trace (or spectrogram) and assume that the streaking spectra at a fixed time delay can be calculated using the so-called strong-field approximation (SFA). For narrow-band pulses with bandwidth of few tens of eVs, one can use the FROG-CRAB (frequency-resolved optical gating for complete reconstruction of attosecond bursts) method [18] to retrieve the spectral phase. This method is not valid for pulse durations typically under 100 as. To overcome the limitation of FROG-CRAB, for broadband pulses, different new characterization methods have been suggested, such as phase retrieval by omega oscillation filtering (PROOF) [19] and Volkov transform generalized projections algorithm (VTGPA) based methods [20, 21]. In our group, we have also developed the PROBP method (phase retrieval of broadband pulses) [22] and its extension PROBP-AC [23] where AC stands for autocorrelation of the streaking spectra.

All of these retrieval algorithms are based on iterative process by matching the measured photoelectron spectrogram to a guessed one from an unknown XUV pulse and an unknown IR field: the program starts with a guessed XUV and an IR pulse to generate a guessed trace, then compare this output trace with the experimental data. The program keeps running until the difference between the guessed and experimental data is small enough. Recently, two experiments have reported attosecond pulses as short as 53 as [24], and 43 as [25], using PROOF and ML-VTGPA retrieval methods, respectively. However, the PROOF method relies on several approximations: that the IR is a monochromatic field, that the field strength of the IR be small, and that the atomic transition dipole moment be independent of photoelectron energy. How such approximations affect the retrieved results are not easily checked. On the other hand, the VTGPA method always starts with a transform-limited pulse, and that the phase in the time domain can be expanded in a power series. Such a procedure may limit the method to near-transform-limited pulses only. Since harmonics are always generated with chirps, for broadband pulses one would have to be able to deal with pulses that have large chirps.

In our previous work, we have developed the PROBP method. In PROBP, the spectral amplitude of the XUV is obtained directly from the XUV-alone photoelectron spectra. The XUV spectral phase, the amplitude and phase of the vector potential of the IR in the time domain are treated as unknown functions. Each of the three unknown functions are expanded in terms of B-spline functions. B-spline functions are generally used to expand a smooth function with a small number of parameters. The PROBP method has been tested for attosecond pulses with spectral bandwidth up to 100 eV where convergence is reached in minutes to hours [22], depending on the bandwidths and the chirps. Recently, attosecond pulses generated by 1850 nm mid-infrared lasers have been reported in [24–26]. In these experiments, photon energies up to three, or to five hundred electron volts were generated, with spectral bandwidth of several hundred eVs. Such soft x-ray (SXR) pulses are streaked in the mid-infrared (MIR) laser field to generate the streaking spectra. It was found that the PROBP method would not converge after tens of hours of computation if the chirp of the pulse is not small. Since harmonics generated are always chirped, and no materials can be found to compensate the chirp over a spectral range of several hundreds eVs, thus it was concluded that even the PROBP is not a practical method for retrieving the phase of such broadband pulses. We have since developed the PROBP-AC method, where AC stands for autocorrelation. The autocorrelation $Q(\tau_1, \tau_2)$ of the streaking trace between two time delays τ_1 and τ_2 is the product of streaking spectra $S(E, \tau_1)$ and $S(E, \tau_2)$ integrated over the photoelectron energy E. It was found that applying the PROBP-AC method to retrieve attosecond pulses directly from $Q(\tau_1, \tau_2)$ can achieve convergence much faster by at least one or two orders of magnitude, and accurate spectral phases can be retrieved. The ACs obtained from the experimental data and from the retrieved pulse also offer a two-dimensional visual comparison of the quality of the retrieval. The PROBP-AC method has been tested over many theoretically generated streaking spectra and has been used in [27] to retrieve the SXR pulses reported in these two recent experiments [24, 25]. As reported in [27], the pulse durations, or more precisely, the spectral phases retrieved by the PROBP-AC method are different from those reported in the original experimental papers [24, 25].

The previous paragraphs addressed the difficulties of retrieving accurate attosecond pulses in the time domain for broadband pulses. Since high order harmonics generated in the soft x-ray region have very low signals and cross sections for single-photon ionization in the soft x-ray region is smaller by two to three orders of magnitude compared to the XUV region, it is generally understood that the signals of the streaking electron spectra are extremely weak, making unfavorable statistics for retrieval. In particular, up to now, all the retrieval methods analyzed only photoelectrons emitted near zero degree along the polarization direction of the pulses. This practice further reduces the signals used for retrieval. Since the retrieval algorithm is based on quantum theory which is statistical in nature, the low counting rates would impose severe limitations on accurate retrieval. While statistics can be improved by taking data for a longer time, ultrafast lasers are known to drift away after some time duration which would also pollute the collected electron spectra.

One possible remedy to improve the statistics is to use streaking electrons over a large angular range with electrons collected using magnetic bottles. This was actually suggested in [21]. In fact, in reference [21], the authors used the VTGPA method to study theoretically how to retrieve spectral phase from such measurements. In view of the limitation of the VTGPA method, in this article, we illustrate how to extend the PROBP and PROBP-AC methods to streaking spectra collected over a large angular range. In the meanwhile, we also evaluate how accurately the zero-degree approximation can be

used to retrieve electrons collected over an angular range (typically at least 15 degrees) that have been used for the phase retrieval.

In streaking experiments the two pulses are both linearly polarized along the same z-direction. For an atom, electrons can be emitted to zero degree only for electrons that have magnetic quantum number $m = 0$. By collecting electrons near zero degree only, one only needs to include ionization from the $m = 0$ states of the atom. Away from zero degree, however, $m \neq 0$ states would also contribute to the streaking spectra. Because of the streaking field, represented by the vector potential $\vec{A}(t)$ of the IR or the MIR, there is no one-to-one correspondence between the electrons emitted in the laser frame and the ones measured in the laboratory frame. This means that the measured electron yields observed in the laboratory frame are generated from all the subshells, including from all of their magnetic sub-states. For larger atoms such as Ar, Kr, and Xe atoms, especially those involving d-shell electrons, contributions from many subshells have to be included, which lead to a significant increase of complexity in the calculations of photoelectron spectra. On the other hand, in view of the even more severe challenges in streaking experiments using broadband pulses, extra complications in the retrieval methods is warranted.

In this article, we first present the extension of the mathematical formalism for PROBP and PROBP-AC to include electrons emitted at nonzero degrees. We then focus on answering two questions. First, we address how accurately the zero-degree approximation can be used to retrieve electrons collected over an angular range (typically at least 15 degrees in experiments). Second, if the streaking electrons are collected over a large angular range in the laboratory frame, can we extend the PROBP and PROBP-AC methods to characterize the spectral phase of broadband pulses? We will also investigate how sensitive the retrieved pulse is to the noise in the experimental data and if the effect of noise is mitigated when electrons are collected from a larger angular region.

This article is organized as follows: section 2 introduces the theoretical background and the relevant mathematical expressions, including the derivation of the angular dependent transition dipole and the SFA model of the streaking measurement. Section 3 discusses how large the collection angle is allowed if the zero-degree approximation is to be used. In section 4 we demonstrate the performance of our method. We conclude this work in section 5. Atomic units are used throughout this article unless mentioned.

2. Angular dependence of the amplitude and phase of the photoelectron wave packet

In this article, we are interested in retrieving an attosecond pulse from angular integrated streaking spectra (AISS). For clarity, we first derive the expression of electron wave packet of a one-electron atom photoionized by an XUV pulse according to elementary perturbation theory. The atomic Hamiltonian is given as

$$H_0 = -\frac{\nabla^2}{2} + V(r). \tag{1}$$

Specifically, we treat a one-electron model, where the electron is under the influence of a model potential $V(r)$ which is parameterized as in Tong and Lin [28] in the form

$$V(r) = \frac{-Z_c + a_1 e^{-a_2 r} + a_3 r e^{-a_4 r} + a_5 e^{-a_6 r}}{r}, \tag{2}$$

here $Z_c = 1$ is the asymptotic charge seen by the electron. The potential in equation (2) can also be expressed as the sum of a Coulomb potential $-1/r$ and a remaining short-range potential. We can solve the time-independent Schrödinger equation numerically to obtain bound state and continuum state wave functions. For the initial state

$$\langle \mathbf{r}|\ \mathrm{i}\rangle = \langle \mathbf{r}|\ n_i l_i m_i\rangle = R_{n_i l_i}(r) Y_{l_i m_i}(\hat{r}), \tag{3}$$

where l_i is the orbital quantum number, m_i is the magnetic quantum number, $R_{nl}(r)$ is the radial wave function, and Y_{lm} is the spherical harmonic. The continuum state $|E\hat{k}\rangle$ in which the emitted photoelectron has energy $E = \frac{k^2}{2}$ and direction $\hat{k}$ can be constructed by partial wave expansion as

$$|E\hat{k}\rangle = \sum_{LM} e^{-i\eta_L(E)} Y^*_{LM}(\hat{k}) |ELM\rangle, \tag{4}$$

$$\langle \mathbf{r}|\ ELM\rangle = R_{EL}(r) Y_{LM}(\hat{r}), \tag{5}$$

where $R_{EL}(r)$ is the energy-normalized radial wave function, $\eta_L(E) = -\frac{L\pi}{2} + \sigma_L(E) + \delta_L(E)$ is the phase shift for the partial wave with angular quantum number L, $\sigma_L = \arg\left[\Gamma\left(L + 1 - iZ_c/k\right)\right]$ is the Coulomb phase shift, and δ_L is the phase shift due to the short-range potential. In spherical coordinates, the direction of the electron momentum $\hat{k}$ can be denoted by the polar angle θ_k and the azimuthal angle φ_k.

Consider one-photon ionization by an XUV pulse. We choose the polarization axis of the light as the z-axis. In frequency domain, the XUV pulse is expressed by $\tilde{E}_{\mathrm{XUV}}(\Omega)$. Based on first-order perturbation theory, one can then write the photoelectron wave packet as

$$\begin{aligned}|\psi(t)\rangle &= \sum_{lm} \int dE \tilde{E}_{\mathrm{XUV}}\left(E + I_p\right) e^{-iEt} \\ &\quad \times \langle Elm|\, z\, |n_i l_i m_i\rangle\, |Elm\rangle \\ &= \int dE \tilde{E}_{\mathrm{XUV}}\left(E + I_p\right) e^{-iEt} \times \\ &\{\langle R_{E,l_i-1}|r|R_{n_i,l_i}\rangle \langle Y_{l_i-1,m_i}|\cos\theta_r|Y_{l_i,m_i}\rangle |E\,(l_i-1)\,m_i\rangle \\ &+ \langle R_{E,l_i+1}|r|R_{n_i,l_i}\rangle \langle Y_{l_i+1,m_i}|\cos\theta_r|Y_{l_i},m_i\rangle |E\,(l_i+1)\,m_i\rangle\}.\end{aligned} \tag{6}$$

Here I_p is the ionization potential of the initial state. In photoelectron measurements, usually one projects this wave packet onto a stationary state $|E\hat{k}\rangle$, that is

$$\langle E\hat{k}|\psi(t)\rangle = \tilde{E}_{\mathrm{XUV}}\left(E + I_p\right) d\left(E, \hat{k}\right) e^{-iEt}. \tag{7}$$

The modulus square of equation (7) gives the photoelectron yield measured in the direction $\hat{k}$. Removing the electric field of the XUV from equation (7), we obtain the complex angular dependent dipole matrix element:

$$\begin{aligned} d(E,\hat{k}) = & e^{i\eta_{l_i-1}(E)} Y_{l_i-1,m_i}(\hat{k}) \\ & \times \langle R_{E,l_i-1}| r |R_{n_i,l_i}\rangle \langle Y_{l_i-1,m_i}| \cos\,\theta_r |Y_{l_i,m_i}\rangle \\ & + e^{i\eta_{l_i+1}(E)} Y_{l_i+1,m_i}(\hat{k}) \\ & \times \langle R_{E,l_i+1}| r |R_{n_i,l_i}\rangle \langle Y_{l_i+1,m_i}| \cos\,\theta_r |Y_{l_i,m_i}\rangle . \end{aligned} \tag{8}$$

While the modulus square of equation (8) can be deduced from single photon ionization measurement, its phase is not available. If the phase can be measured, then we can say that the full electron wave packet from the simple photoionization experiment by the known attosecond pulse is completely determined.

To simplify the analysis, take Ne atom as the target, where $n_i = 2$ and $l_i = 1$. Denote the radial matrix elements as $W_L(E) = \langle R_{EL}|r|R_{21}\rangle$. By working out the angular part, we obtain

$$\begin{aligned} d_0(E,\hat{k}) = & \sqrt{\frac{1}{12\pi}} \left\{ W_0(E) e^{i\eta_0(E)} \right. \\ & \left. + W_2(E) e^{i\eta_2(E)} \left(3\cos^2\theta_k - 1\right) \right\} \end{aligned} \tag{9}$$

for the case where the initial state has $m_i = 0$. For the initial state with $m_i = \pm 1$, we have

$$d_{\pm 1}(E,\hat{k}) = \pm\sqrt{\frac{3}{8\pi}} W_2(E) e^{i\eta_2(E)} \cos\,\theta_k \sin\,\theta_k e^{\pm i\varphi_k}. \tag{10}$$

For streaking experiments, according to strong-field approximation, the photoelectron spectrum at an ejection angle θ_k at time delay τ is given by

$$\begin{aligned} S(\mathbf{p},\tau) = & \frac{1}{3} \sum_{m=-1,0,1} \left| \int_{-\infty}^{\infty} E_{\mathrm{XUV}}(t-\tau) d_m[\mathbf{k}(t)] \right. \\ & \left. \times e^{-i\int_t^{\infty} \left(pA(t')\cos\theta_k + \frac{1}{2}A^2(t')\right) dt'} e^{i\left(\frac{p^2}{2} + I_p\right)t} dt \right|^2 . \end{aligned} \tag{11}$$

This expression simplifies for $\theta_k = 0^\circ$ or 180°. In the two special cases, only the $m_i = 0$ channel contributes to the electron spectrum. For $\theta_k = 0^\circ$, the trace takes this form,

$$\begin{aligned} S(\mathbf{p},\tau) = & \left| \int_{-\infty}^{\infty} E_{\mathrm{XUV}}(t-\tau) d_0[k(t)] \right. \\ & \left. \times e^{-i\int_t^{\infty} \left(pA(t') + \frac{1}{2}A^2(t')\right) dt'} e^{i\left(\frac{p^2}{2} + I_p\right)t} dt \right|^2 . \end{aligned} \tag{12}$$

This is the familiar expression for the streaking spectra at zero degree.

The angle integrated streaking spectra (AISS) is defined by

$$S_{\mathrm{AISS}}(E,\tau,\theta_{\max}) = \int_0^{\theta_{\max}} S(E,\tau,\theta_k) \sin(\theta_k)\, d\theta_k, \tag{13}$$

where $\theta_{\max}$ is the upper limit of the collection angle.

3. Accuracy of phase retrieval in the zero degree approximation

First, we investigate the zero-degree approximation, which has been commonly used in the retrieval applications so far. We take Ne as the target throughout this work instead of Kr [26] or Xe [25] used in experiments, where ionization from s−, p− and d−shells should be considered. Note that for each orbital angular momentum ℓ, all the $2\ell+1$ magnetic substates should be included for electrons ejected at nonzero angles. For ionization from Ne, we include the three magnetic substates $m_i = 0$, -1 and $+1$ of the 2p orbital since photoionization cross sections from 2s and 1s states are much smaller. Thus, the angular dependent streaking trace is proportional to the sum of the three pathways:

$$S(E,\theta_k,\tau) \propto |d_0|^2 + |d_{-1}|^2 + |d_{+1}|^2, \tag{14}$$

of the three m_i states. From equation (10), we can see $|d_{-1}| = |d_{+1}|$, thus equation (14) can be re-written as

$$S(E,\theta_k,\tau) \propto |d_0|^2 + 2|d_1|^2. \tag{15}$$

The angular dependent amplitude of dipole $|d_0|$ and $\sqrt{2}\,|d_1|$ are shown in figures 1(a) and (b). Both ionization pathways exhibit strong angular dependence. The $|d_0|$ has a minimum around $\theta_k = 57^\circ$. The origin of this minimum can be found in equation (9). In Ne atom, $W_2(E) \gg W_0(E)$ in the whole energy region. As a result, $|d_0|$ is dominated by the second term of equation (9): $W_2(E)\, e^{i\eta_2} \left(3\cos^2\theta_k - 1\right)$ except when the angle-dependent term goes to zero. This occurs at $\theta_k = 57^\circ$. Similarly, from equation (10) we can find that the minimum of $\sqrt{2}\,|d_{\pm 1}|$ is at $\theta_k = 0^\circ$ and 90°. The cross sections are symmetric with respect to 45°.

We next compare the contribution of pathways $|d_0|$ and $\sqrt{2}\,|d_1|$ vs the ejection angle of the photoelectrons, see figure 2(b). It is clear that $|d_0| \gg \sqrt{2}\,|d_1|$ if $\theta_k < 10^\circ$. In figure 2(a), the difference between the zero degree dipole $|d_0(\theta_k = 0)|$ and $|d_0(\theta_k)|$ is presented. It is clear that $|d_0(\theta_k)| \approx |d_0(\theta_k = 0^\circ)|$ if $\theta_k < 10^\circ$. Thus, we can conclude that if $\theta_{\max} < 10^\circ$, we have

$$\begin{aligned} S_{\mathrm{AISS}}(E,\tau,\theta_{\max}) & \approx \sum_{\theta_k=0}^{\theta_{\max}} S(E,\tau,\theta_k) \sin\,\theta_k \\ & \approx S(E,\tau,\theta_k = 0^\circ) \sum_{\theta_k=0}^{\theta_{\max}} \sin\,\theta_k \end{aligned} \tag{16}$$

and thus the zero degree approximation is valid.

In streaking experiments, one always collects all electrons within an angular range, i.e., one always measures AISS, see equation (13). Because of the $\sin\,\theta_k$ factor in the integrand of this equation, one would prefer to choose a large $\theta_{\max}$ so that there are 'enough' counts in the data for retrieval. In figures 3 and 4 we investigate how much error would incur if we extend

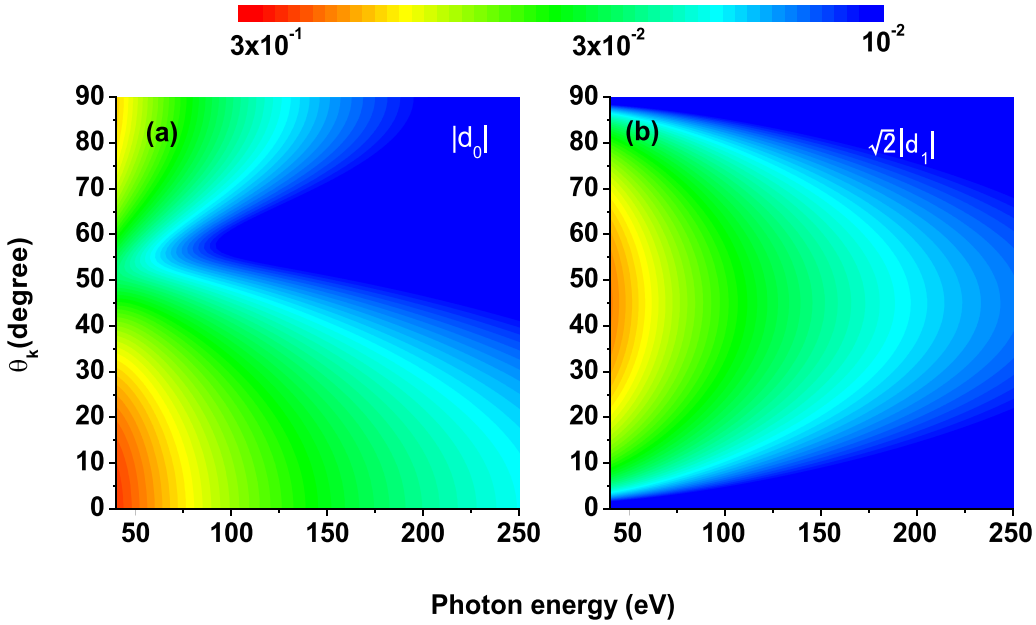

Figure 1. Calculated angular dependence of single-photon ionization dipole transition amplitude (a) $|d_0(E,\theta_k)|$ for $m_i = 0$ and (b) $\sqrt{2}\,|d_1(E,\theta_k)|$ for $m_i = 1$ and -1, for ionization from the 2p magnetic sub-states of Ne. They are calculated from equations (9) and (10) where the radial matrix element and phase for each partial wave $L = 0$ and 2 are calculated from solving the time-independent Schödinger equation.

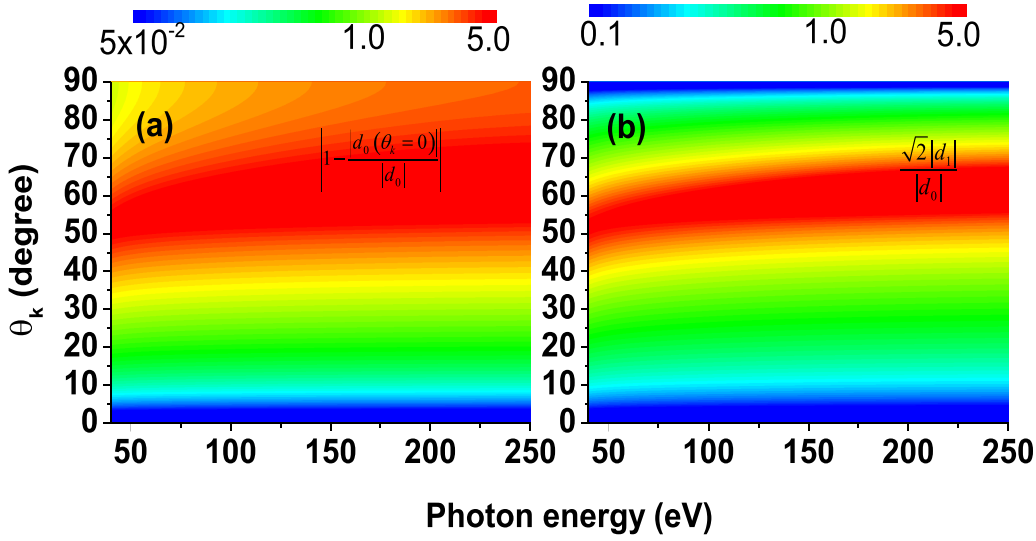

Figure 2. (a) Normalized deviation of $\left|1-\frac{|d_0(\theta_k=0)|}{|d_0|}\right|$ vs photon energy E and ejection angle θ_k in photoionization from 2p shell of Ne. (b) Measure of relative transition dipole amplitude $\frac{\sqrt{2}|d_1|}{|d_0|}$ for total $m_i = 1$ and -1 with respect to $m_i = 0$ vs photon energy E and ejection angle θ_k.

θ_{max} to 15° and 35°, for narrow and broadband pulses, respectively. In figure 3, we use an XUV pulse which takes a Gaussian form with a central photon energy of 60 eV and a full width at half maximum (FWHM) bandwidth of 10 eV to generate the input trace using equation (13), the IR field is 800 nm in wavelength, cosine squared envelope, four cycles in total duration, 10^{12} W cm^{-2} in peak intensity, and the carrier-envelope phase (CEP) is zero. Figure 3(a) shows the input spectral phase of the XUV pulse that is to be compared with results retrieved using the PROBP under the zero degree approximation for $\theta_{max} = 10$, 15, 35 degrees, respectively. From figure 3(a), the spectral phases derived from using 10 and 15 degrees agree well with the input phase, but the one from 35° shows significant discrepancies. This behavior is also reflected in intensity of attosecond pulses in the time domain, as seen in figure 3(b). In terms of pulse duration (FWHM), the input and the retrieved durations using different θ_{max} are shown in table 1. It should be mentioned, however, a pulse duration does not provide the

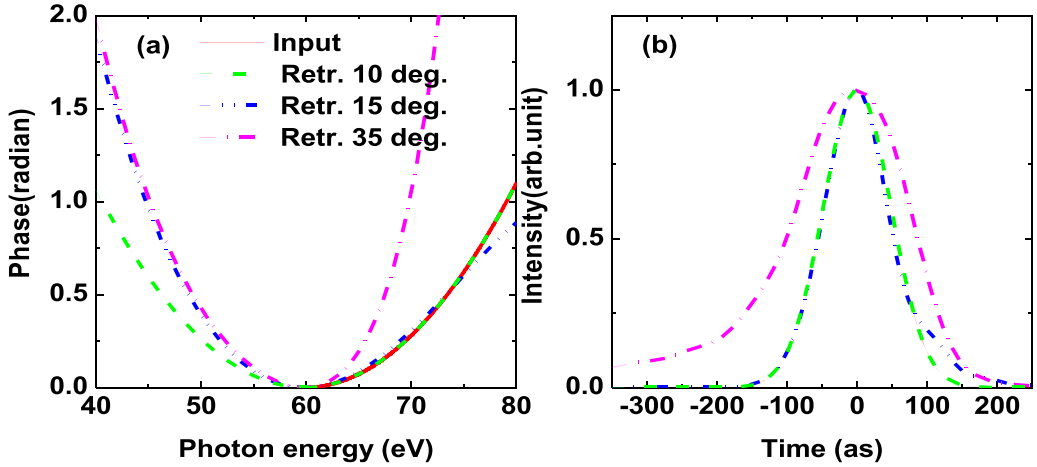

Figure 3. Dependence of the retrieved phase (a) and the temporal intensity (b) of the XUV pulses with the maximal collection angles of 10, 15 and 35°, respectively. Zero degree approximation is used. The retrieved XUV phase and time-domain intensity show that zero degree approximation is valid for collection angles of 10 and 15 degrees, but fails when the collection angle is extended to 35°. The PROBP method is used for the retrieval in this example. In this figure, we use an XUV pulse which takes a Gaussian form with a central photon energy of 60 eV and a full width at half maximum (FWHM) bandwidth of 10 eV to generate the input trace using equation (13).

Table 1. Investigation of the validity of the zero degree approximation. The input XUV has a full-width at half-maximum (FWHM) of 116 as. The 'experimental' AISS are collected over $\theta_{\max} = 10$, 15 and 35 degrees, respectively. Note that the 'experimental' data are calculated from equation (11), but the retrieval uses equation (12). The PROBP method is used to obtain the results in this table. The table shows that at 15° collection angle, zero-degree approximation is still acceptable.

	Input FWHM (as)	Output FWHM (as)	Error
$\theta_{\max} = 10°$	116	118	0.017
$\theta_{\max} = 15°$	116	122	0.052
$\theta_{\max} = 35°$	116	214	0.845

full description of an attosecond pulse. Instead, both the amplitude and phase, either in the energy domain or time domain, should be fully specified for a genuine characterization of an attosecond pulse.

Next we show the test for broadband pulses. The central photon energy of the XUV pulse is 200 eV with an FWHM bandwidth of 100 eV, the streaking field is an MIR laser with wavelength of 2000 nm and 10^{12} W cm^{-2} in peak intensity. For such a broadband pulse, the PROBP method converges slowly or unable to converge, and thus we use the PROBP-AC method. The conclusions, as shown in figure 4 and table 2, are similar to figure 3 and table 1, respectively. However, the $\theta_{\max}$ effect is more significant. Because of the larger bandwidth, the chirp of the phase within the bandwidth is larger, thus making the wing (away from the center of the pulse) drops more slowly. Figure 4(b) shows that for $\theta_{\max} = 15°$ we can see oscillatory tails not seen when $\theta_{\max} = 10°$. For $\theta_{\max} = 35°$, the retrieved pulse is essentially wrong, deeming the zero-degree approximation not valid. Figure 4(a) shows that for this case the retrieved spectral phase is completely wrong, thus the retrieved electric field in the time domain would be completely incorrect.

4. Phase retrieval using streaking spectra collected over a large angular range

In this section, we discuss the other question raised in this work: can we accurately retrieve the spectral phase if we use streaking spectra collected over a broad angular range for better statistics? For this purpose, we firstly show how the AISS in equation (13) changes with $\theta_{\max}$.

Figure 5 shows the streaking spectra versus the time delay, for four different values of $\theta_{\max}$. One can see small differences but the major difference lies in the magnitude of the spectra (the range of the color scale for each figure increases with an increasing $\theta_{\max}$). To provide a more quantitative comparison, we define a new variable $P(\theta_{\max}, \tau) = \int_0^\infty S_{\rm AISS}(E, \tau, \theta_{\max})\, dE$, where $S_{\rm AISS}$ is the streaking spectrum with photoelectron angle θ_k integrated from zero to $\theta_{\max}$. As shown in figure 6, $P(\theta_{\max}, \tau)$ increases monotonically from small to large $\theta_{\max}$. This figure also says that by limiting $\theta_{\max}$ to 10 or 15 degrees, the electron yields indeed is much smaller than when $\theta_{\max}$ is taken to be larger than 60 degrees. For example, if the collection angle is 90 degrees, only about 24% of the counts coming from below 20 degrees. To retrieve the spectral phase from the streaking spectra collected over a large angular region, one can no longer use equation (12) which accounts for ionization from $m_{\rm i} = 0$ magnetic state only. One would have to calculate the electron spectra using equation (11) which includes contribution from all the magnetic substates. Since contribution from $+m_{\rm i}$ and $-m_{\rm i}$ states are identical, the number of calculations for a given ℓ is ℓ+1. This would increase the computational load only linearly.

To demonstrate that one can accurately retrieve XUV pulses using electrons emitted over a larger angular range, we perform a calculation taking the case for $\theta_{\max} = 35°$. We have shown that at this angle, the zero-degree approximation is not valid. Figure 7 shows two examples, one for the

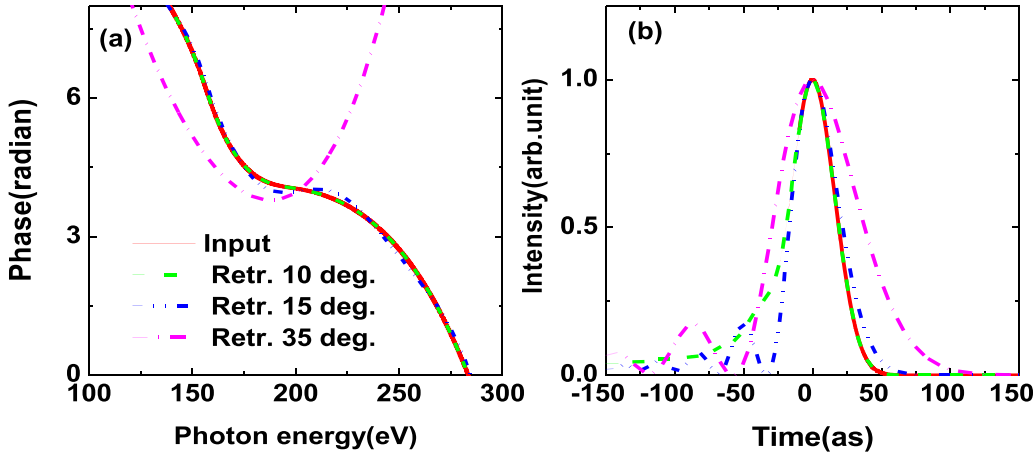

Figure 4. Similar study as in figure 3 but for a broadband pulse. The central energy of the SXR pulse is 200 eV and the bandwidth is 100 eV. The MIR field has wavelength of 2000 nm. In (b), it shows there already exists some errors for the zero degree approximation if the collection angle is 15°. If the collection angle is 35°, the zero degree approximation fails miserably, especially the retrieved phase, see (a). The PROBP-AC method is used for the phase retrieval in this figure.

Table 2. Similar study as in table 1 but for a broadband SXR pulse to test the validity of zero-degree approximation. The input chirped SXR pulse has an FWHM of 32 as. For collection angles of 10 and 15°, the zero degree approximation is valid but not for a collection angle of 35°. The PROBP-AC method is used.

	Input FWHM (as)	Output FWHM (as)	Error
$\theta_{\max} = 10°$	32	32	0.00
$\theta_{\max} = 15°$	32	33	0.03
$\theta_{\max} = 35°$	32	65	1.03

narrow-band XUV pulse and another for the broadband SXR pulse. For the former, the XUV central energy is at 60 eV and the bandwidth is 10 eV. The IR field is 800 nm in wavelength and four optical-cycle long, and a cosine squared envelope is used. The input spectral phase of the XUV is shown in figure 7(a). Using equation (11) to generate the streaking spectra and equation (13) to calculate the AISS, we take the results as 'experimental' data. For the retrieval, we use the PROBP method. We assume that the spectral phase is not known and that both the amplitude and phase of the vector potential $\vec{A}$ of the IR are not known. From PROBP we obtain the spectral phase of the XUV. It is compared to the input phase in figure 7(a) and good agreement in the intensity in the time domain has also been retrieved, see figure 7(b).

To test the retrieval for the broadband pulse, we consider the SXR central energy is at 200 eV, and the FWHM bandwidth is 100 eV. MIR laser with wavelength of 2000 nm is used for the streaking field. The input spectral phase of the SXR is given in figure 7(c). We use PROBP-AC method to retrieve the broadband pulse. As seen from figures 7(c) and (d), both the spectral phase and the time-domain intensity of the SXR have been accurately retrieved.

Using AISS spectra for retrieval clearly would take more time since electron spectra at many angles and from many initial magnetic substates have to be calculated. Without optimizing the codes so far, in the present example, the computer time is about a factor of 35 more compared to calculations under the zero-degree approximation. (It will take six hours to make the retrieval using equations (11) and (13) for $\theta_{\max} = 35°$). When actual experimental data become available and the community are interested in accurate characterization of attosecond pulses, the codes will be optimized for the users.

Next, we investigate how the noise in the streaking spectra would affect the retrieved spectral phase or the temporal profile of the attosecond pulse. For this purpose, we assign the maximum random error (both plus and minus) is ten percent of the maximum of the streaking spectra at zero degree. Such random error is applied to photoelectron spectra at each energy, angle and time delay. If the resulting signal becomes negative, the signal is set to zero. With a known input attosecond pulse, we generate the streaking spectra at each E, τ and θ_k as before. We then add a random noise $N(E, \tau, \theta_k)$ to each point with the maximum noise as described above. We then obtain the 'experimental' angle-integrated streaking spectra according to $S_{\rm AISS}(E, \tau, \theta_{\max}) = \int_0^{\theta_{\max}} [S(E, \tau, \theta_k) + N(E, \tau, \theta_k)] \sin\theta_k d\theta_k$. We then follow the retrieving procedure outlined above to demonstrate that the retrieved spectral phase will become closer to the input one as the streaking photoelectrons are collected with increasing angular range.

Figure 8 demonstrates the results of such a study using a broadband pulse. The central photon energy is set at 200 eV, the full width at half maximum (FWHM) bandwidth is 100 eV which would give a pulse duration of 20 as if the pulse is transform-limited. We chose a spectral phase [see figure 8(b)] such that the input pulse has duration of 320 as. The mid-infrared laser field for streaking has wavelength of 2000 nm, four optical cycle in total duration and a cosine squared envelope. For such broadband pulse, the PROBP-AC method was used to retrieve the pulse.

In figure 8(a), we show the intensity profile of the input attosecond pulse and the retrieved ones when the 'experimental' streaking spectra were collected up to 10, 30 and 70 degrees, respectively. The corresponding results for the spectral phase are shown in figure 8(b). If the collection angles are up to 10 degrees, the retrieved pulse duration is 276

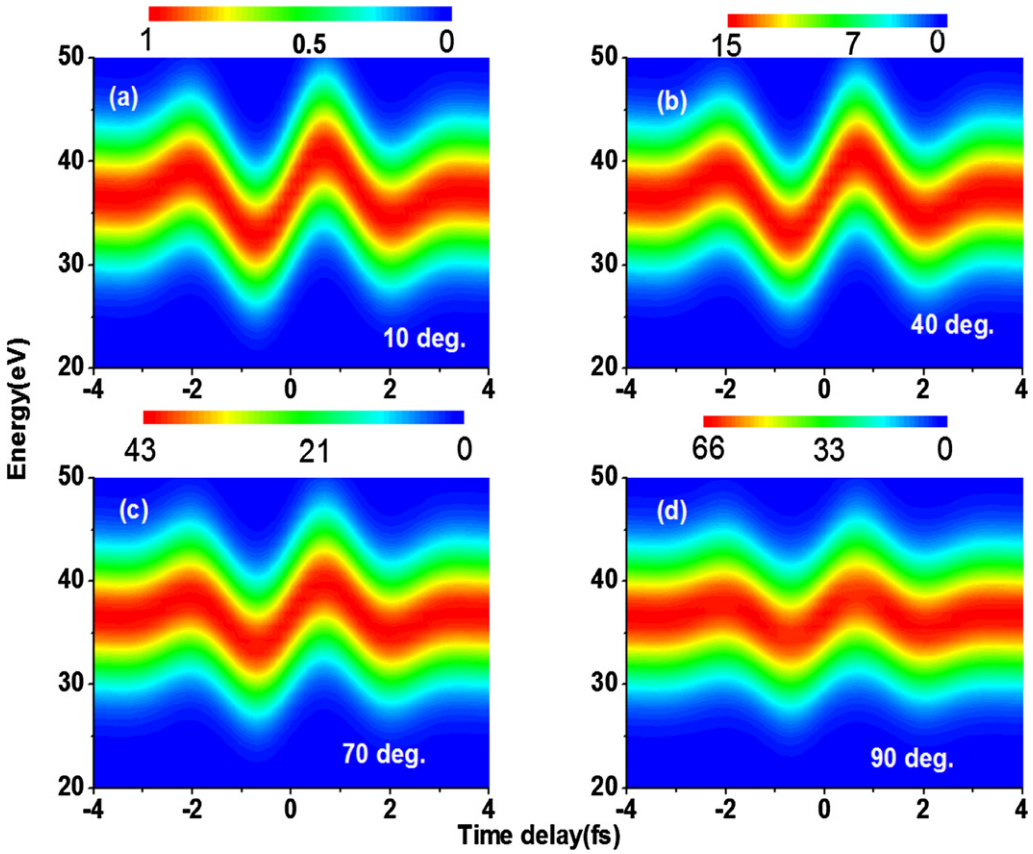

Figure 5. (a–d) The streaking spectra collected over different angular range for $\theta_{\max}$ of 10, 40, 70 and 90°, respectively. The streaking spectra show little change except for the increase of yield as the collection angle is increased (see the color bars for magnitudes). Central energy of the XUV is 60 eV and bandwidth is 10 eV. The IR is 800 nm.

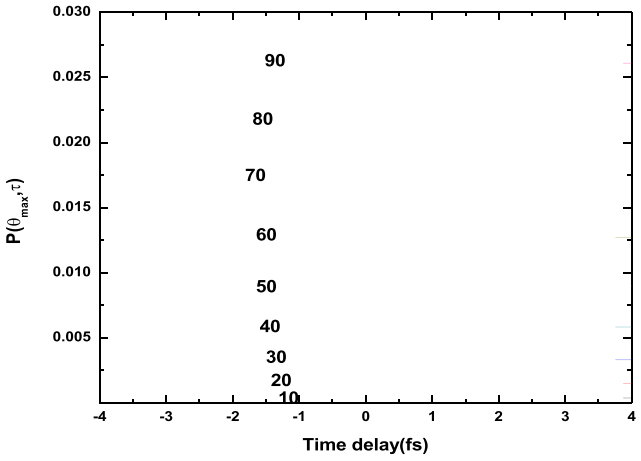

Figure 6. Energy and angle integrated streaking spectra $P(\theta_{\max}, \tau)$ versus time delay for various collection angles (10, 20, …, and 90°). The main effect of increasing $\theta_{\max}$ is the increase of the strength of the AISS.

as. If the collection angles extend to 30 degrees, the retrieved pulse duration is 290 as. If the collection angle is up to 70 degrees, then the retrieved pulse duration is 300 as. These results demonstrate that indeed the use of streaking spectra collected from a larger angular range would improve the accuracy of the retrieved results. This owes much to the fact shown in figure 6 where it is shown that the integrated streaking spectra intensities increase rapidly with larger collection angles while the 'noises' increase at the constant rates.

We remark that most experiments are able to collect photoelectrons over a large angular range in streaking experiments, but often only electrons at small angles, typically up to 10 or 15 degrees, are used for the phase retrieval analysis. This has the advantage that one can use equation (12) for the phase retrieval. If the angle-integrated streaking spectra is extended to larger angles, then one has to use the more complicated equation (11) for the phase retrieval. However, as demonstrated in this article, this can be carried out using the PROBP or PROBP-AC method without significant increase of computational efforts.

It should also be mentioned here that, although our conclusion is based on the calculations of Ne target, the method is directly applicable to other targets.

5. Discussion and conclusions

In this work, we aimed to answer two questions in attosecond pulse characterization: first, what is the applicable range of the so called zero degree approximation? Second, can we mitigate the noise effect by using streaking spectra collected over a larger angular region? For this purpose, we modify our recently developed PROBP and PROBP-AC methods

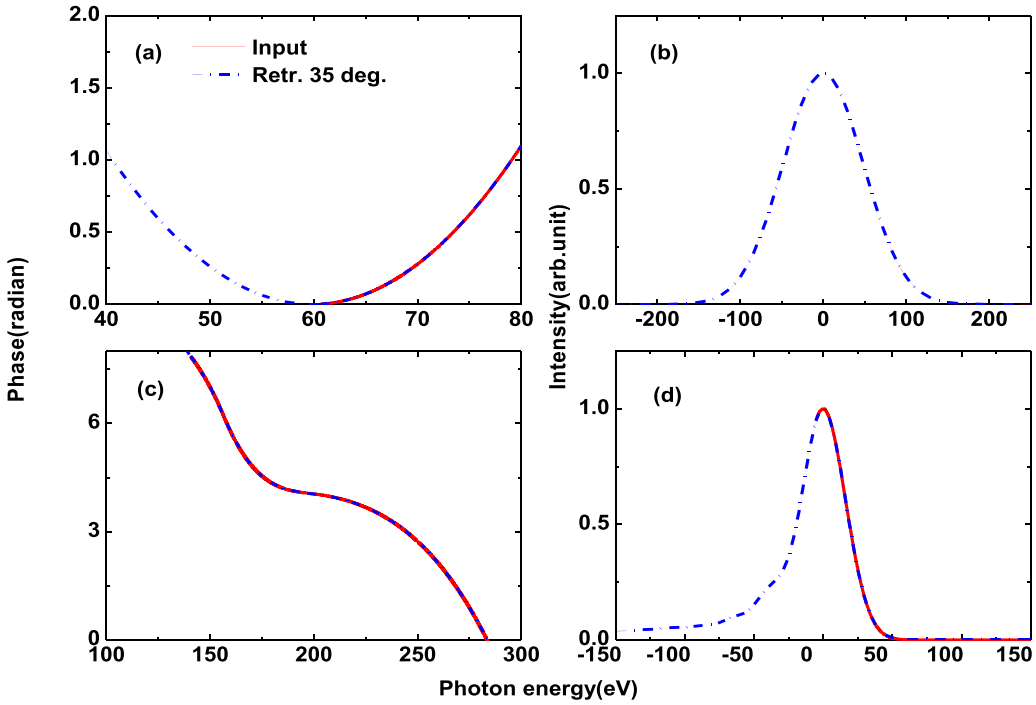

Figure 7. Retrieval of phase (a), (c) and temporal intensity (b), (d) from AISS with $\theta_{max} = 35°$. These figures are to be compared with figures 3 and 4 where the pulses are retrieved using the zero degree approximation. Using equation (11) for the retrieval, we show that the XUV or SXR pulses can be accurately retrieved from angle-integrated streaking spectra. Results shown in (a) and (b) are obtained using PROBP, and results shown in (c) and (d) are obtained using PROBP-AC method.

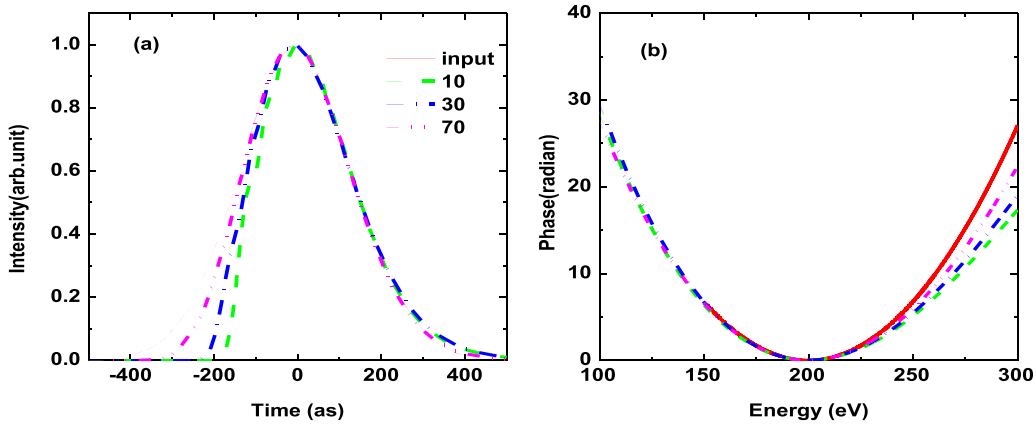

Figure 8. Retrieval of phase (a) and temporal intensity (b) from angle-integrated streaking spectra for different maximal collection angle θ_{max}. The XUV pulse takes a Gaussian form with central photon energy of 200 eV and a full width at half maximum (FWHM) bandwidth of 100 eV (20 as if the pulse is transform limited). The MIR field is 2000 nm in wavelength, cosine squared envelope and four optical cycles in total duration. The input chirped XUV pulse has an FWHM of 320 as. We use equation (13) to calculate the streaking trace. We add a random noise to each point of the trace to generate the 'experimental' data (see text). The PROBP-AC method is used for the phase retrieval.

for retrieving attosecond pulses from angular integrated streaking traces. Based on the numerical and mathematical analysis, we find that zero degree approximation is valid if θ_{max} is below 10 degrees. The effect of noise can be reduced by including electrons from larger angles. By accounting for the angular dependence of the streaking spectra correctly in the retrieval algorithm within the SFA, the PROBP and PROBP-AC can be extended to accurately retrieve the spectral phase of broadband SXR pulses.

Acknowledgments

This research was supported in part by the Chemical Sciences, Geosciences, and Biosciences Division, Office of Basic Energy Sciences, Office of Science, US Department of Energy, under Grant No. DE-FG02-86ER13491. XZ was also supported by the National Natural Science Foundation of China under Grant No. 11904192. CW was supported by the National Natural Science Foundation of China under Grant No. 11964028.

ORCID iDs

Xi Zhao https://orcid.org/0000-0003-3114-5416

References

[1] Hentschel M *et al* 2001 Attosecond metrology *Nature* **414** 509–13

[2] Drescher M *et al* 2002 Time-resolved atomic inner-shell spectroscopy *Nature* **419** 803–7

[3] Lin C D, Le A T, Jin C and Wei H 2018 *Attosecond and Strong-Field Physics Principles and Applications* (Cambridge: Cambridge University Press)

[4] Schiffrin A *et al* 2013 Optical-field-induced current in dielectrics *Nature* **493** 70–4

[5] Cavalieri A L *et al* 2007 Attosecond spectroscopy in condensed matter *Nature* **449** 1029–32

[6] Calegari F *et al* 2014 Ultrafast electron dynamics in phenylalanine initiated by attosecond pulses *Science* **346** 336–9

[7] Colosimo P *et al* 2008 Scaling strong-field interactions towards the classical limit *Nat. Phys.* **4** 386–9

[8] Vozzi C, Calegari F, Benedetti E, Gasilov S, Sansone G, Cerullo G, Nisoli M, De Silvestri S and Stagira S 2007 Millijoule-level phase-stabilized few-optical-cycle infrared parametric source *Opt. Lett.* **32** 2957–9

[9] Popmintchev T *et al* 2012 Bright coherent ultrahigh harmonics in the keV x-ray regime from mid-infrared femtosecond lasers *Science* **336** 1287–91

[10] Takahashi E J, Kanai T, Ishikawa K L, Nabekawa Y and Midorikawa K 2008 Coherent water window x-ray generation by phase-matched high-order harmonic generation in neutral media *Phys. Rev. Lett.* **101** 253901

[11] Ishii N, Kaneshima K, Kitano K, Kanai T, Watanabe S and Itatani J 2014 Carrier-envelope phase-dependent high harmonic generation in the water window using few-cycle infrared pulses *Nat. Commun.* **5** 3331

[12] Cousin S L, Silva F, Teichmann S, Hemmer M, Buades B and Biegert J 2014 High-flux table-top soft x-ray source driven by sub-2-cycle, CEP stable, 1.85 μm 1 kHz pulses for carbon K-edge spectroscopy *Opt. Lett.* **39** 5383–6

[13] Schmidt B E *et al* 2010 Compression of 1.8 μm laser pulses to sub-two optical cycles with bulk material *Appl. Phys. Lett.* **96** 121109

[14] Stein G J *et al* 2016 Water-window soft x-ray high-harmonic generation up to the nitrogen K-edge driven by a kHz, 2.1 μm OPCPA source *J. Phys. B: At. Mol. Opt. Phys.* **49** 155601

[15] Silva F, Teichmann S M, Cousin S L, Hemmer M and Biegert J 2015 Spatiotemporal isolation of attosecond soft x-ray pulses in the water window *Nat. Commun.* **6** 6611

[16] Teichmann S M, Silva F, Cousin S L, Hemmer M and Biegert J 2015 0.5-keV soft x-ray attosecond continua *Nat. Commun.* **7** 11493

[17] Li J, Ren X, Yin Y, Cheng Y, Cunningham E, Wu Y and Chang Z 2016 Polarization gating of high harmonic generation in the water window *Appl. Phys. Lett.* **108** 231102

[18] Mairesse Y and Quéré F 2005 Frequency-resolved optical gating for complete reconstruction of attosecond bursts *Phys. Rev.* A **71** 011401

[19] Chini M, Gilbertson S, Khan S D and Chang Z 2010 Characterizing ultrabroadband attosecond lasers *Opt. Express* **18** 13006–16

[20] Keathley P D, Bhardwaj S, Moses J, Laurent G and Kärtner F X 2016 Volkov transform generalized projection algorithm for attosecond pulse characterization *New J. Phys.* **18** 073009

[21] Gaumnitz T, Jain A and Wörner H J 2018 Complete reconstruction of ultra-broadband isolated attosecond pulses including partial averaging over the angular distribution *Opt. Express* **26** 14719–40

[22] Zhao X, Wei H, Wu Y and Lin C D 2017 Phase-retrieval algorithm for the characterization of broadband single attosecond pulses *Phys. Rev.* A **95** 043407

[23] Yu W, Zhao X, Wei H, Wang S J and Lin C D 2019 Method for spectral phase retrieval of single attosecond pulses utilizing the autocorrelation of photoelectron streaking spectra *Phys. Rev.* A **99** 033403

[24] Li J *et al* 2017 53-attosecond x-ray pulses reach the carbon K-edge *Nat. Commun.* **8** 186

[25] Gaumnitz T, Jain A, Pertot Y, Huppert M, Jordan I, Lamas F A and Wörner H J 2017 Streaking of 43-attosecond soft-x-ray pulses generated by a passively CEP-stable mid-infrared driver *Opt. Express* **25** 27506–18

[26] Cousin S L, Di Palo N, Buades B, Teichmann S M, Reduzzi M, Devetta M, Kheifets A, Sansone G and Biegert J 2017 Attosecond streaking in the water window: a new regime of attosecond pulse characterization *Phys. Rev.* X **7** 041030

[27] Zhao X, Wang S J, Yu W, Wei H and Lin C D 2020 Metrology of time-domain soft x-ray attosecond pulses and re-evaluation of pulse durations of three recent experiments *Phys. Rev. Appl.* **13** 034043

[28] Tong X M and Lin C D 2005 Empirical formula for static field ionization rates of atoms and molecules by lasers in the barrier-suppression regime *J. Phys. B: At. Mol. Opt. Phys.* **38** 2593